

# SCAN-ANGLE ENHANCEMENT OF QUASI-STATIC PIEZOELECTRIC MEMS MIRROR BY MULTIPLE RING-SHAPED DESIGN AND CROSS-ELECTRODE ARRANGEMENT

Hung-Yu Lin<sup>1,3</sup>, Hao-Chien Cheng<sup>1,3</sup>, Mingching Wu<sup>3</sup>, Jerwei Hsieh<sup>4</sup>,  
Mei-Feng Lai<sup>1,2</sup>, and Weileun Fang<sup>1,2</sup>

<sup>1</sup> Inst. of NanoEng. and MicroSyst., National Tsing Hua University, TAIWAN

<sup>2</sup> Dept. of Power Mech. Eng., National Tsing Hua University, TAIWAN

<sup>3</sup> Coretronic MEMS Corporation, TAIWAN and

<sup>4</sup> Asia Pacific Microsystems, Inc., TAIWAN

## ABSTRACT

This study presents a novel quasi-static MEMS scanner featuring multiple ring-shaped actuators, designed to achieve angle enhancement through multiple scan angle accumulation. The proposed design has three merits: (1) multiple ring-shaped actuators (torque-generator): accumulating the scan-angle from outer/middle/inner ring-shaped actuators, (2) driving electrodes arrangement: enhancing angle accumulation to improve total scan-angle, (3) large reflective mirror size (3 mm×2 mm): enhancing laser beam scanning (LBS) image projection quality. Thus, large scan angle at quasi-static actuation is achieved. Measurements demonstrate the scanner has an optical scan angle of 18-degree (mechanical scan angle of ±4.5-degree) at the quasi-static actuation of 60/120 Hz with a unipolar driving voltage of 80 V. Compared with existing scanners, performances of presented design are competitive in figure-of-merit (FOM, optical-scan-angle × mirror-size ( $\theta \times D$ )).

## KEYWORDS

MEMS, micro-mirror, piezoelectric, quasi-static

## INTRODUCTION

MEMS scanners can be used in various LBS applications, such as LiDAR (light detecting and ranging) [1], pico-projectors [2], AR glasses [3]. The MEMS micro-mirror is a competitive option to realize LiDAR and projection system, owing to the features of miniaturization and batch fabrication. In general, the wide Field of View (FOV) and high refresh rate are important specifications for display applications. Thus, large mirror size and wide scan angle are preferred for quasi-static micro-mirror design. However, the trade-off between a large aperture and wide-angle scanning is a design concern. Moreover, quasi-static mirrors face challenges in achieving large-angle scanning due to the absence of resonant effect that could amplify the scan angle.

To date, various actuation mechanisms, including electrostatic [4], electromagnetic [5], and piezoelectric [6] approaches, have been reported for driving MEMS micro-mirrors. The electrostatic method offers the advantage of a relatively simple and mature fabrication process but is limited by the pull-in effect and the need for high driving voltage. The electromagnetic approach provides a large driving force but is hindered by issues such as joule heating and complex assembly requirements. Among existing

technologies, piezoelectric MEMS scanners offer advantages such as lower driving voltage, no pull-in effect, and no need for complex assembly. In contrast, piezoelectric actuation, using materials like lead zirconate titanate (PZT), stands out for its ability to generate a large driving force, enabling wide scanning angles. Additionally, piezoelectric MEMS scanners benefit from lower driving voltage. With advancements in process technologies, piezoelectric actuation has emerged as a promising solution for MEMS scanning mirrors [7].

To address the issue of insufficient scanning angle in quasi-static mirrors, making it suitable for LBS displays, this study presents a piezoelectric MEMS scanner. The proposed design integrates multi-ring-shaped actuators with electrical-routing arrangements. These actuators function as torque generators, enabling the accumulation of angular movements contributed by each actuator through torsional springs. Furthermore, the electrical-routing design enhances the driving efficiency of the actuators, achieving both a large scan angle and a large aperture.

## DESIGN AND MODELING

The proposed micro-scanner (chip footprint: 7 mm × 5.3 mm, reflective area: 3 mm × 2 mm) features a design integrating multi-ring actuators, pivotal connections,

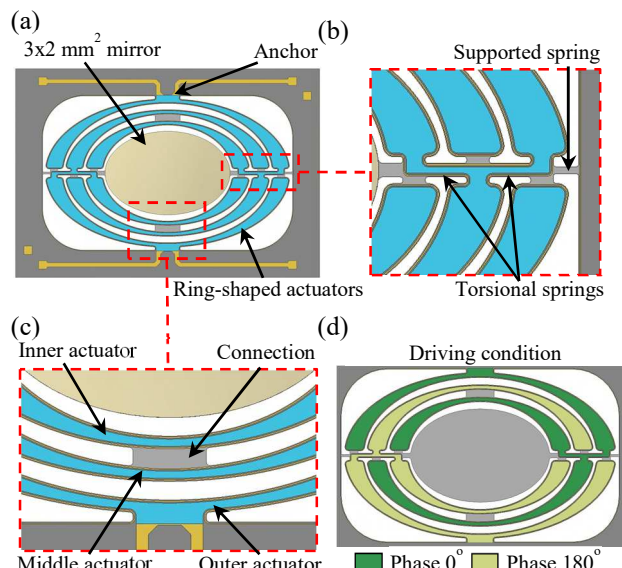


Figure 1: Design concepts, (a) the design of the proposed scanning mirror, (b) zoom-in of springs structure of mirror device, (c) zoom-in of actuators and connection structures of mirror device, (d) the proposed electrical-routing arrangement.

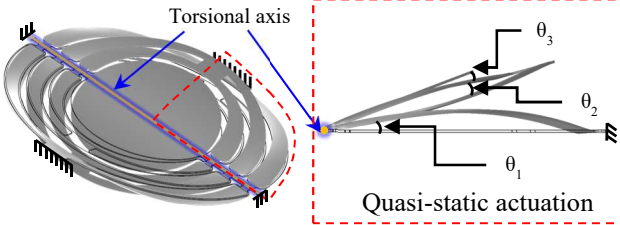


Figure 2: The deflection profiles of mirror and actuators driven by the proposed electrical-routing design.

torsional springs, supportive springs, and an elliptical mirror (Figs. 1a-b). The actuators are arranged in multiple ring shapes (Fig. 1c), consisting of outer, middle, and inner actuators. The ring-structures are connected/fixed to anchors/connections (acting as pivots), enabling each actuator to function as an independent torque generator. Moreover, the proposed micro-scanner employs the electrical-routings design in Fig. 1d to enhance the driving performance of the ring-shaped actuators. The unique cross-side electrical-routing arrangement enables better deflection configurations of the ring structures, ensuring efficient actuator performance. Fig. 2 further illustrates the superposition of scanning angles achieved during quasi-static actuation. The angles  $\theta_1$  and  $\theta_3$  are generated by the outer and inner actuators respectively, while  $\theta_2$  is contributed by the middle actuator. Notably, the angular accumulation depends on the curvature of each actuator. For instance, the middle actuator must bend in the opposite direction to the outer and inner actuators; otherwise, its contribution would be  $-\theta_2$  instead of  $\theta_2$ . To reduce the impact of residual stress on the reflective area, the PZT layer was removed from the center of the mirror. This design refinement reduces stress effects that could impact scanning performance.

Fig. 3 shows the simulation results of the proposed design, the piston-mode is at 1.7 kHz, the 1<sup>st</sup> and 2<sup>nd</sup> tilting-modes are respectively at 1.4 kHz and 4.7 kHz. Simulations in Fig. 4 further depict the difference of scanning angles achieved by two electrical-routing designs. Fig. 4a displays the reference (left) and proposed (right) electrical-routing designs. The deflection profiles of actuators driven by the proposed electrical-routings design match well with the result shown in Fig. 2, so that a larger scan angle is achieved. This configuration is essential to achieving a larger scanning angle and consistent angular superposition in the same direction.

Fig. 4b shows scan-angle responses at different driving voltages under quasi-static actuation, highlighting the arrangement. For the presented multiple ring-shaped actuators, the proposed electrical-routing arrangement (red-dot) achieves over 70% better scan angle than the

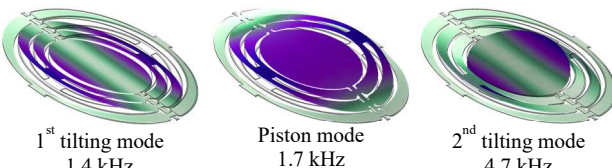


Figure 3: Simulation modal analysis results of resonant tilting & piston mode shapes and frequencies of proposed design.

reference arrangement (blue-dot) during quasi-static actuation. This substantial improvement demonstrates the efficacy of the ring-shaped actuators and optimized routing, making it a compelling solution for quasi-static requiring wide-angle scanning.

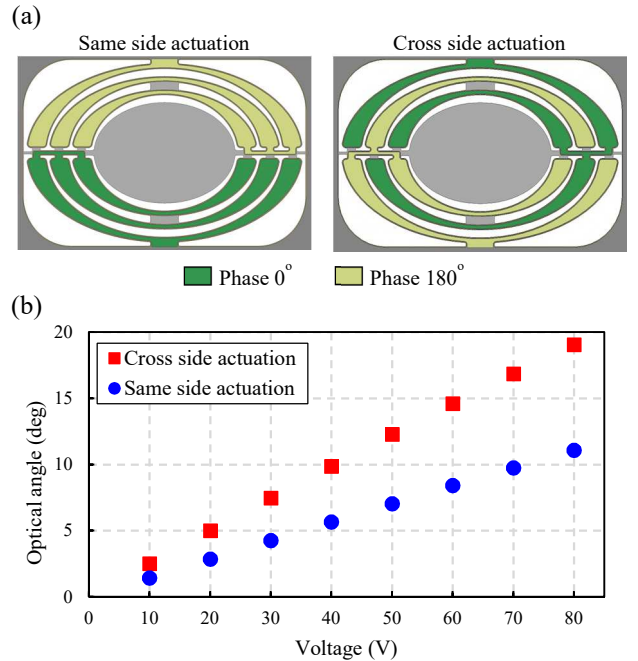


Figure 4: Schema and comparison of two driving methods.

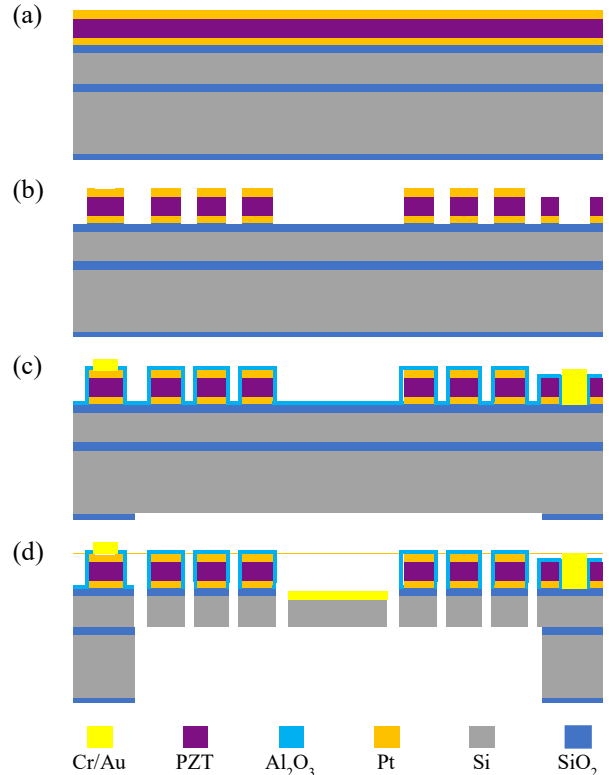


Figure 5: Simplified cross-sectional process flow of the fabricated MEMS micro-mirrors, (a) deposition of all functional layers, (b) patterning the piezoelectric PZT layer and both electrodes, (c) deposition and patterning of passivation layer, (d) device release after front-side and back-side definition.

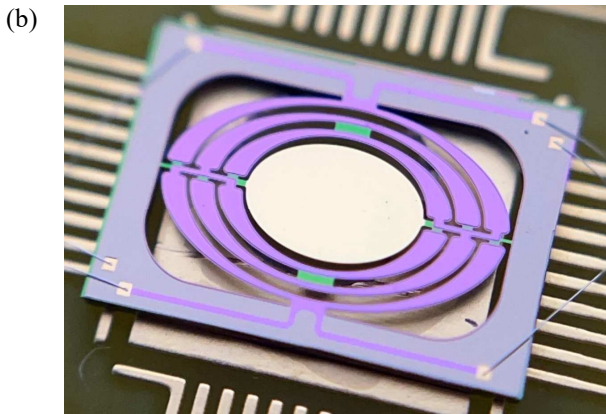
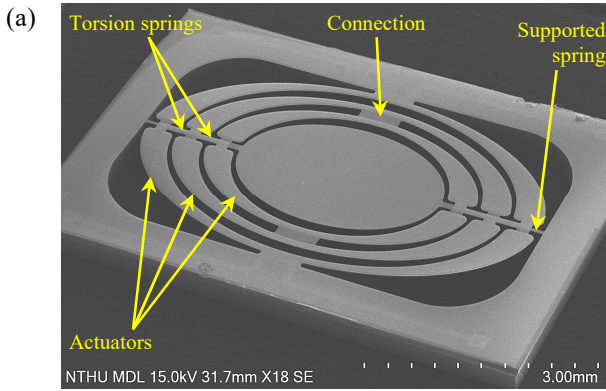


Figure 6: Fabrication results, (a) SEM micrographs of the scanner, (b) scanner chip after wired-bonded on PCB.

## FABRICATION

Figure 5 illustrates the fabrication processes for creating the mirror on a 6-in SOI wafer with a 15  $\mu\text{m}$  thick device layer. As shown in Fig. 5a, in addition to PZT film, the Pt layers were deposited on the substrate to function as the top and bottom electrodes. In Fig. 5b, the top electrode, PZT, and bottom electrode were patterned using the RIE process. Next, as depicted in Fig. 5c, an  $\text{Al}_2\text{O}_3$  film was deposited via atomic layer deposition (ALD) to serve as a passivation layer, protecting the piezoelectric material from environmental moisture. The passivation layer was then patterned using RIE to expose the contact area of the top electrode, followed by deposition and patterning of the metal film. Moreover, the oxide layer on the backside was patterned to define the suspended region. Finally, in Fig. 5d, the passivation and oxide layers were etched to outline the reflective area, and the device Si layer was patterned with front-side DRIE. A two-step DRIE process was then applied to create the rib-reinforcement structure. After that, the buried oxide was etched to release the structure, and a reflective metal layer was deposited onto the mirror plate using a shadow mask.

Fabrication results are presented in Fig. 6. Micrographs in Fig. 6a reveal typical fabricated micro-mirror chip of proposed design. Fig. 6b shows the chip wire-bonded on printed circuit board (PCB) for testing.

## MEASUREMENTS AND DISCUSSIONS

Measurements in Fig. 7 show the frequency responses of the scanning mirror. The resonant frequencies of the micro-scanner are measured by the Laser-Doppler

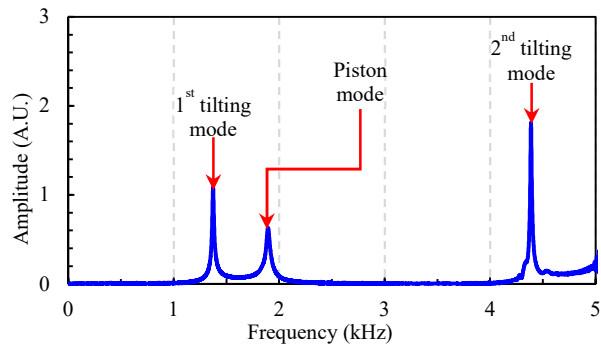


Figure 7: frequency response by LDV.

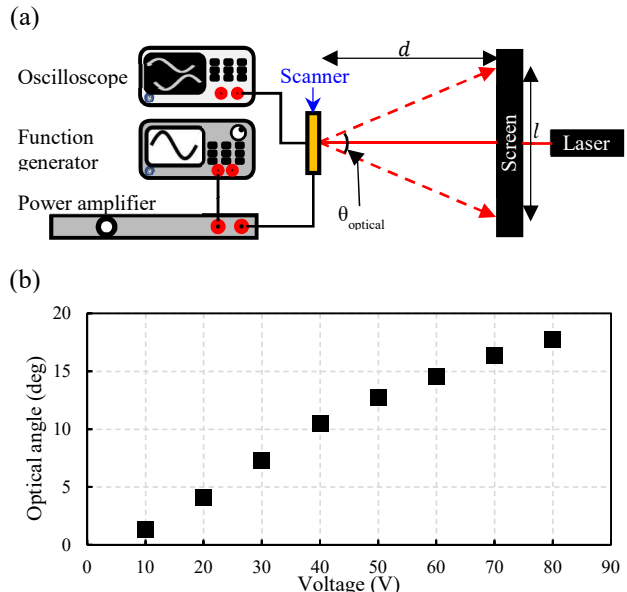


Figure 8: measurement results (a) system setup, (b) optical scan angle with different voltage.

Vibrometer (LDV), capturing the vibrational modes from 0 to 5 kHz. The 1<sup>st</sup>/2<sup>nd</sup> tilting modes are observed at 1.5 kHz/4.4 kHz, respectively, while the piston mode occurs at 1.9 kHz. Moreover, the scan-angle test setup was conducted with the device-under-test (DUT) placed perpendicular to the laser source, as illustrated in Fig. 8a. Reflected laser light from the MEMS mirror is projected onto a perforated sheet, enabling precise optical angle measured from reflect-light length on screen. Measurements in Fig. 8b show optical scan angles for different unipolar driving voltages. The results show a maximum optical scan angle of approximately 18-degree (mechanical scan angle of 4.5-degree) during quasi-static actuation. The scan angle shows a linear response to driving voltages, also demonstrates stable performance, with consistent actuator response enhancing the angular movement of the mirror.

Figure 9 provides a comparative analysis of the FOM values for various micro-scanners, including the proposed design. The FOM, defined as the product of the optical scan angle ( $\theta$ ) and mirror size (D), evaluates performance across different voltages. The proposed design (as highlighted in red) demonstrates a highly competitive FOM compared to existing piezoelectric quasi-static micro scanners, effectively achieving large-angle scanning within compact dimensions.

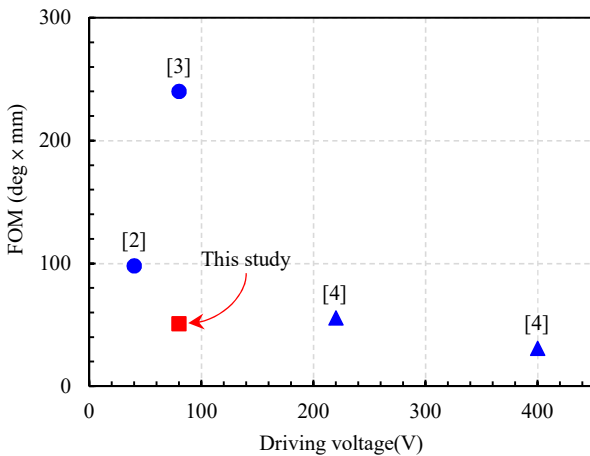


Figure 9: Comparison with existing piezoelectric quasi-static scanner [8-10].

## CONCLUSIONS

A wide angle, large aperture ( $3 \text{ mm} \times 2 \text{ mm}$ ) quasi-static piezoelectric MEMS mirror has been realized. The proposed novel multi ring-shaped actuators can consistently superimpose angular movement of the mirror. Also, the presented electrical-routing design enables better deflection configurations of the actuators, particularly the middle actuator, which exhibits opposite curvature under quasi-static actuation. Simulation results further validate the design's effectiveness. The deflection profiles achieved by the proposed electrical-routing arrangement align closely with the desired performance, resulting in scan angles over 70% larger during quasi-static actuation. The proposed scanner driving at 60/120 Hz under 80 V also shows competitive FOM, with 18-degree optical scan angle and  $3 \text{ mm} \times 2 \text{ mm}$  mirror size. Furthermore, the presented performance almost meets the requirement of quasi-static mirror in high resolution.

## ACKNOWLEDGEMENTS

This project was supported by the National Science and Technology Council of Taiwan under grant number NSTC 111-2221-E-007 -070 -MY3, NSTC 111-2221-E-007 -070 -MY3, NSTC 112-2622-E-007 -023, NSTC 113-2221-E-007 -055 -MY2. The authors also appreciate the Center for Nanotechnology, Materials Science and Microsystems (CNMM) of National Tsing Hua University, Semiconductor Research Institute, Taiwan (TSRI), Nano-Electro-Mechanical-System Research Center of National Taiwan University, Taiwan (NEMS), and Nano Facility Center (NFC) of National Yang Ming Chiao Tung University, Coretronic MEMS Corporation, Asia Pacific Microsystems, Inc. and MA-tek for providing the process tools and experiment instrument.

## REFERENCES

- [1] B. Jiang, M. Peng, Y. Liu, T. Zhou, and Y. Su, "The fabrication of 2D micromirror with large electromagnetic driving forces," *Sensors and Actuators A: Physical*, vol. 286, pp. 163-168, 2019.
- [2] A. C.-L. Hung, H. Y.-H. Lai, T.-W. Lin, S.-G. Fu, and M. S.-C. Lu, "An electrostatically driven 2D micro-scanning mirror with capacitive sensing for projection display," *Sensors and Actuators A: Physical*, vol. 222, pp. 122-129, 2015.
- [3] N. Boni, R. Carminati, G. Mendicino, M. Merli, D. Terzi, B. Lazarova, and M. Fusi, "Piezoelectric MEMS mirrors for the next generation of small form factor AR glasses," *MOEMS and Miniaturized Systems XXI*, vol. 12013, pp. 30-46, 2022.
- [4] M. Wu, H.-Y. Lin, and W. Fang, "A poly-si-based vertical comb-drive two-axis gimbaled scanner for optical applications," *IEEE Photonics Technology Letters*, vol. 18, no. 20, pp. 2111-2113, 2006.
- [5] H.-A. Yang, T.-L. Tang, S. T. Lee, and W. Fang, "A novel coilless scanning mirror using eddy current Lorentz force and magnetostatic force," *Journal of Microelectromechanical Systems*, vol. 16, no. 3, pp. 511-520, 2007.
- [6] H.-C. Cheng, S.-C. Liu, H.-Y. Lin, C.-C. Hsu, F. Shih, K.-C. Liang, M. Wu, M.-F. Lai and W. Fang, "On the design of piezoelectric MEMS scanning mirror for large reflection area and wide scan angle," *Sensors and Actuators A: Physical*, vol. 349, p. 114010, 2023.
- [7] R. Gabai, G. Cahana, M. Yehiel, G. Yearim, T. Yusupov, A. Baram and M. Naftali, "The return of the interlace," *Optical Architectures for Displays and Sensing in Augmented, Virtual, and Mixed Reality (AR, VR, MR) III*, vol. 11931, pp. 203-209, 2022.
- [8] N. Boni, R. Carminati, G. Mendicino and M. Merli, "Quasi-static PZT actuated MEMS mirror with  $4 \times 3 \text{ mm}^2$  reflective area and high robustness," *MOEMS and Miniaturized Systems XX*, vol. 11697, pp. 42-52, 2021.
- [9] N. Boni, R. Carminati, G. Mendicino, M. Merli, D. Terzi, B. Lazarova and M. Fusi, "Piezoelectric MEMS mirrors for the next generation of small form factor AR glasses," *MOEMS and Miniaturized Systems XXI*, vol. 12013, pp. 30-46, 2022.
- [10] C. Stoeckel, M. Katja, M. Marcel, A. Agnè, Z. Sven, F. Roman, H. Karla and K. Harald, "Static high voltage actuation of piezoelectric AlN and AlScN based scanning micromirrors," *Micromachines*, vol. 13, no. 4, pp. 625, 2022.

## CONTACT

\*W. Fang, Tel:+886-3-5742923; fang@pme.nthu.edu.tw